fMRI Activation during Observation of Others' Reach Errors

Nicole Malfait[1,2], Kenneth F. Valyear[1], Jody C. Culham[1], Jean-Luc Anton[3], Liana E. Brown[4], and Paul L. Gribble[1]

Abstract

■ When exposed to novel dynamical conditions (e.g., externally imposed forces), neurologically intact subjects easily adjust motor commands on the basis of their own reaching errors. Subjects can also benefit from visual observation of others' kinematic errors. Here, using fMRI, we scanned subjects watching movies depicting another person learning to reach in a novel dynamic environment created by a robotic device. Passive observation of reaching movements (whether or not they were perturbed by the robot) was associated with increased activation in fronto-parietal regions that are normally recruited in active reaching. We found significant clusters in parieto-occipital cortex, intraparietal sulcus, as well as in dorsal premotor cortex. Moreover, it appeared that part of the network that has been shown to be engaged in processing self-generated reach error is also involved in observing reach errors committed by others. Specifically, activity in left intraparietal sulcus and left dorsal premotor cortex, as well as in right cerebellar cortex, was modulated by the amplitude of observed kinematic errors. ■

INTRODUCTION

When the kinematics of limb movement are perturbed by altered force environments (Sainburg, Ghez, & Kalkanis, 1999; Lackner & Dizio, 1994; Shadmehr & Mussa-Ivaldi, 1994), somatosensory as well as visual error signals may drive adaptive update of the motor command. Indeed, adaptation may develop in complete absence of vision, solely on the basis of somatosensory feedback (e.g., Dizio & Lackner, 1995, 2000; Scheidt, Reinkensmeyer, Conditt, Rymer, & Mussa-Ivaldi, 2000; Sainburg, Ghilardi, Poizner, & Ghez, 1995), whereas visual information can partially compensate for missing proprioceptive feedback, as in the case of large fiber neuropathy for instance (Ghez, Gordon, & Ghilardi, 1995; Sainburg et al., 1995). Several motor control studies have investigated how visual and proprioceptive estimates of hand-path error are combined to drive adaptation of reaching movements (e.g., Scheidt, Conditt, Secco, & Mussa-Ivaldi, 2005; Sober & Sabes, 2003). Although this work is aimed at better understanding the integration of multimodal sensory information about self-generated error, recent research in motor learning has attempted to link these principal findings and ideas to the visual processing of errors committed by others (Van Schie, Mars, Coles, & Bekkering, 2004).

Since the original report of neurons in the macaque monkey brain that respond to both action execution and action observation (Di Pellegrino, Fadiga, Fogassi, Gallese, & Rizzolatti, 1992), later dubbed "mirror neurons" (Gallese, Fadiga, Fogassi, & Rizzolatti, 1996), there has been growing interest in the role of mirror neurons and action observation in motor learning (Cross, Kraemer, Hamilton, Kelley, & Grafton, 2009; for reviews, see Iacoboni & Mazziotta, 2007; Kilner, Friston, & Frith, 2007) and cognition (for reviews, see Rizzolatti & Fabbri-Destro, 2008; Rizzolatti & Craighero, 2004). Although there has been some controversy about the mirror system in the human brain (reviewed in Dinstein, Thomas, Behrmann, & Heeger, 2008), a recent fMRI adaptation study provides evidence that action execution and action observation are encoded in the same neural populations within the human brain (Chong, Cunnington, Williams, Kanwisher, & Mattingley, 2008). Neuromagnetic stimulation (Maeda, Kleiner-Fisman, & Pascual-Leone, 2002; Hari et al., 1998) and neuroimaging studies (Rizzolatti, Fogassi, & Gallese, 2001; Iacoboni et al., 1999) suggest that visual observation of actions may directly activate sensorimotor structures implicated in the active production of the observed actions (for reviews, see Shmuelof & Zohary, 2007; Fadiga, Craighero, & Olivier, 2005; Rizzolatti & Craighero, 2004). Today, a growing body of evidence strongly suggests that mechanisms involved in learning by observing might be very similar to some of those engaged in learning by actual doing (Cross et al., 2009; Flanagan & Johansson, 2003; Petrosini et al., 2003; Blandin & Proteau, 2000). Thus, the question has been raised about whether processing our own motor errors engages the same neural mechanisms as those involved in learning from watching other people

[1]University of Western Ontario, London, Ontario, Canada, [2]UMR 6149 Neurosciences Intégratives et Adaptatives, CNRS, Marseille Cedex, France, [3]Centre IRMf de Marseille, Marseille Cedex, France, [4]Trent University, Peterborough, Ontario, Canada

commit similar errors. Using event-related potentials, Van Schie et al. (2004) demonstrated that in a choice reaction task, similar cortical regions are activated in response to self-generated errors as in response to errors committed by another person.

Mattar and Gribble (2005) showed that not only can information used in the movement-selection planning stage be acquired through observation, information relevant to movement execution can also be visually conveyed. Subjects who observed a video depicting another person learning to reach in a novel force environment, created by a robotic device, performed better when later tested in the same environment, as compared with subjects who observed similar but unperturbed movements. In the present study, we used fMRI to explore which neural structures might be involved in processing reach errors committed by others. Consistent with recent findings (Filimon, Nelson, Hagler, & Sereno, 2007), passive observation of reaching movements (whether or not they were perturbed by novel forces) activated fronto-parietal structures known to be active during visually guided reaching. Moreover, we found convergence between the regions whose activity correlated with the kinematic error in the observed hand-paths and areas that have been suggested to be engaged in processing self-generated active reach errors.

METHODS

Participants

Fourteen neurologically intact individuals (age range = 19–29 years with mean of 25 years, 7 women) participated in the study. All were right-handed, had normal or corrected-to-normal vision, and were naive to the goals of the study. Each participant provided informed consent according of procedures approved by the University of Western Ontario Health Sciences Review Ethics Board.

Experimental Setup

Subjects were presented with video clips using a PC laptop connected to a video projector. Recordings were made using a digital video camera, edited using Final Cut Pro 4 software, and presented using Macromedia Flash MX 6.0. The movies were shown on a rear-projection screen which straddled the subject's waist while they lay supine in the MRI scanner. Subjects viewed the screen through a mirror mounted to the top of the head coil. At a viewing distance of approximately 120 cm, the images subtended approximately 5° of visual angle.

Stimulus Videos

Video recordings depicted an individual making a series of reaching movements while holding the handle of a robotic device (Interactive Motion Technologies, Cambridge, MA). A top–down view (see Figure 1A) was provided in which the right arm of an actress was shown reaching from a central position to a single 15-cm distant target. Movement direction was either 90° (outward) or −90° (inward) relative to the frontal plane of the actress. A stationary fixation point was superimposed on the arm image at the location of movement start (see Figure 1A). A superimposed image of the target turned yellow to trigger movement onset, and provided information about movement duration at the end of the reaching movement. Specifically, when the target was reached within 500 ± 50 msec, it was extinguished. When the movement was too slow (>550 msec), it turned green. For reaches that were too fast (<450 msec), it turned red. Each video clip showed a series of seven movements from the central start position to one of the two targets and back (the same target was used throughout the seven trials; movement direction changed across video clips). The target-reaching phase (reaction time, hand displacement, and stabilization at the target) lasted 1 sec. The robot was programmed so that 1 sec after target onset it brought the hand of the person shown in the movie back to the central position, which took 3.55 sec. Thus, each individual back-and-forth movement lasted 4.55 sec and each video clip lasted 32 sec (7 × 4.55 + 150 msec initial delay).

Three different types of 32-sec video clips were assembled. "Force-field" (FF) movies depicted movements performed as the robot applied perturbing forces. "Null-field" (NF) movies showed movements performed as the robot was inactive (motors turned off). Each of the seven trials in an NF epoch was based on a separate clip such that the movements were highly similar but not identical. "Scrambled" (S) movies were used as a baseline condition, and were made up from the NF movies as follows. Each image of the NF movies was divided into a grid of 24 × 24 cells. Aside from two individual cells that were kept at their original locations, all cells of the grid were then randomly reordered. The two cells that remained unchanged corresponded to the fractions of the image that displayed the movement starting point (where the stationary fixation point was superimposed) and the target (see Figure 1B). This type of scrambling preserved the low-level motion features of the display (including direction and velocity), while making the details of the action (e.g., the motions of shoulder and elbow joints) incoherent. For all (FF, NF, and S) movie types, each 32-sec clip displayed either reaches outward to the 90° target, or reaches inward to the −90° target.

Each 32-sec clip was obtained as follows. The actress performed four separate blocks of 50 movements: two sets in the FF environment (one set in each direction; outward or inward) and two sets in the NF environment (again, one in each direction). From each of the four 50-movement recordings, two series of seven movements were then extracted, from which two condition-wise equivalent 32-sec video clips were built. In particular,

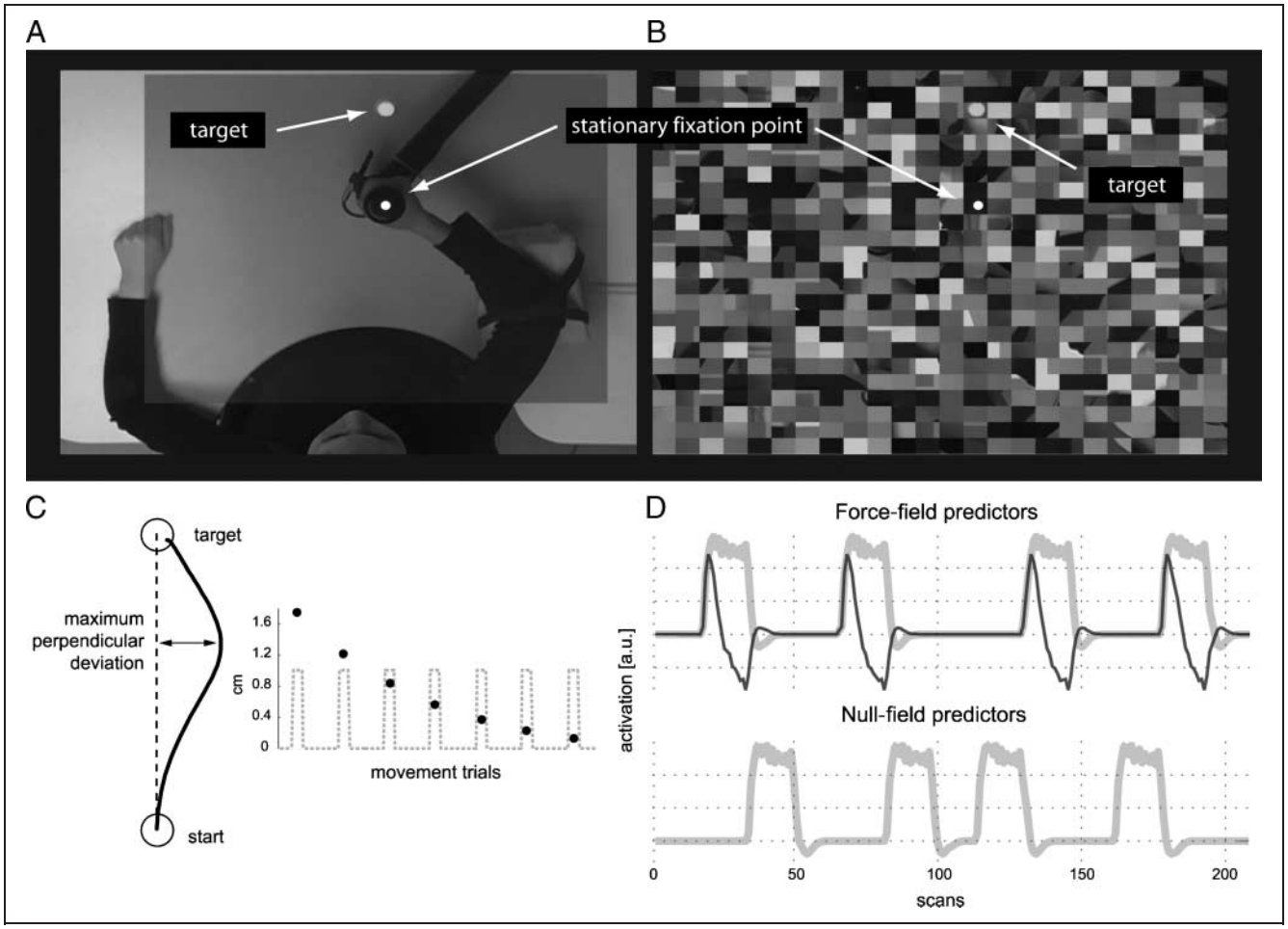

Figure 1. (A) Subjects watched movies presenting a top view of another person reaching to a visual target either in a "null field" (NF) or in a "force field" (FF). (B) As baseline condition, scrambled versions of the movies were shown. (C) Kinematic error was quantified as the maximum perpendicular deviation from a straight line connecting the start position and target. The first movements in the FF were perturbed, but the kinematic error decreased rapidly throughout the trials. The gray dotted line corresponds to the reaches, and the black dots show the corresponding hand-path deviations. (D) For one run, the two convolved "reach-observation" predictors (NF and FF conditions) are in gray. The black line corresponds to the convolved Dirac "deviation-parameter" function. This (centered) predictor was added to model neural activation for the FF condition.

the FF movements were selected so as to reflect accelerated but smooth learning sequences. Initial movements were curved and late movements were straight. To avoid the potentially confounding situation in which FF movements would have both larger spatial errors and more frequent temporal errors, trials were selected so as to equate the number of movements of different durations (<450, 500 ± 50, or >550 msec) across the different movie types (FF, NF, and S). We had two different sequences of different movement durations; one for each of the two sets of FF, NF, and S clips (i.e., the two condition-wise equivalent sets of clips). A total of twelve 32-sec clips were obtained: 2 Sets × 3 Movie types × 2 Movement directions.

Each run was made of 13 clips (total duration: 6 min 56 sec), starting with the S baseline condition (4 FF, 4 NF, and 5 S). Clip-type order was counterbalanced across four different run sequences. For each NF or FF condition, either outward or inward reaches were displayed. Two sets of four sequences were assembled; in the first set, movements performed in the FF were made to the outward target, whereas movements in the NF were to the inward target. The reverse was true for the second set. Subjects received one of the two sets of four run sequences twice.

Task

For all three conditions (NF, FF, and S), participants were instructed to press a key with their left index finger each time the actress completed a movement within the right time (500 ± 50 msec); that is, each time the target turned off when reached. They were asked, while focusing on the movement duration feedback provided by the color-changing target, to keep fixating the stationary fixation dot throughout each run. The visual fixation point was superimposed on the central start position. We chose this

location as it ensured that participants could always see both the upper and lower targets without making eye movements.

Subjects received each run order twice; that is, each subject underwent eight functional runs. Movement directions were balanced across subjects. Half of the subjects saw inward reaching movements during the FF condition and outward reaching movements during the NF condition, whereas the other half saw outward reaching movements during the FF condition and inward reaching movements during the NF condition.

Subject Training outside the Scanner

At least 1 day before the experiment, subjects were trained outside the magnet. They were first trained to perform actual reaching movements while holding the robotic arm. This was intended to orient subjects to the manipulandum and the speed–accuracy feedback. Subjects did not get any experience with force fields; their only experience with the robot was limited to the null field. Under NF condition, they performed two sets of 30 movements to each of the 90°-outward and −90°-inward targets. Subjects' starting posture was comparable to that of the actress shown in the movies (i.e., ~45° at the shoulder and ~90° at the elbow). Subjects were told about how the color-changing target provided feedback about movement duration, and were asked to maximize the number of movements completed within the appropriate time. The subjects were then trained (same session) for the task they would perform in the magnet (see above).

Imaging Procedures

Images were collected at the Robarts Research Institute (London, Ontario, Canada) using a 4-T whole-body MRI system (Varian-Siemens, Palo Alto, CA and Erlangen, Germany) and a full-volume radio-frequency head coil. Each imaging session comprised eight functional runs and a single high-resolution anatomical scan. Functional volumes were collected using a T2*-weighted, segmented (navigator-corrected), 3-D spiral multishot acquisition (echo time [TE] = 15 msec; flip angle [FA] = 40°; repetition time [TR] = 1000 msec with two segments/plane for a volume acquisition time of 2 sec) to image the BOLD signal over time. Each volume acquisition covered 17 continuous, 6-mm quasi-axial slices, ranging from the most superior point of cortex down through ventral fusiform cortex, including approximately ¾ of the cerebellum. The imaging field of view was set at 22.0 × 22.0 cm, with an in-plane resolution of 64 × 64 pixels, resulting in a voxel size of approximately 3.4 × 3.4 × 6.0 mm. We chose to use 6 mm slice thickness due to tradeoffs in spatial and temporal resolution given the limitations of the 4-T scanner. We wanted to acquire full brain coverage from the very top of the brain (e.g., dorsal parieto-frontal cortices) down to the cerebellum without an excessively long volume time (TR = 2 sec). High-resolution anatomical volumes were collected using a T1-weighted 3-D magnetization-prepared FLASH acquisition (inversion time [TI] = 1300 msec; TE = 3.0 msec; TR = 50 msec; FA = 11°). Resultant voxel size was 0.9 × 0.9 × 2.0 mm.

Analysis Approaches

We used both whole-brain voxelwise analyses and ROI approaches to analyze the data. Despite debates regarding the "best" approach (Friston, Rotshtein, Geng, Sterzer, & Henson, 2006; Saxe, Brett, & Kanwisher, 2006), both approaches offer complementary advantages. In short, voxelwise approaches allow the investigation of the whole brain without prior assumptions about spatial localization, whereas ROI approaches can better withstand intersubject variability in sulcal and functional neuroanatomy and can be used to investigate time courses without prior assumptions (particularly with regard to the hemodynamic response function [HRF]). Convergence between the two approaches can bolster the interpretation of the data.

Whole-brain Voxelwise Analysis

fMRI data were analyzed with SPM5 software (Wellcome Department of Cognitive Neurology, London, UK; www.fil.ion.ucl.ac.uk/). The first six functional volumes of each block were removed to eliminate nonequilibrium effects of magnetization. The 208 images of each run were spatially realigned to the first image with a six-parameter rigid-body transform to correct for head movements. Realignment parameters were checked to ensure there had been no large abrupt movements. Even gradual movements throughout the full session were small (<1.5 mm in 12 of 14 subjects; <3 mm in the other 2 of 14 subjects), thus no subjects were removed from the dataset due to excessive head motion. Data were high-pass filtered with a cutoff frequency of 1/128 sec to remove slowly varying trends. The functional images and the anatomical scans were then normalized into a standard stereotaxic space using the MNI template. The functional images were spatially smoothed with an isotropic Gaussian filter (6 mm full width at half maximum). The event-related statistical analysis was performed according to the general linear model, using the standard HRF provided by SPM5. To control for possible noise artifacts in the data, we used a weighted least-squares approach, down weighting images with high noise variance (Diedrichsen & Shadmehr, 2005; www.bangor.ac.uk/~pss412/imaging/robustWLS.html).

Each target-directed reach was modeled as a 1-sec duration event; for each force condition, we included in the design matrix a "reach-observation predictor" that was high during reaching to the target and low otherwise. For the FF-observation condition, we added a second orthogonal "deviation predictor" that accounted for kinematic error independently of activation across all trials of that condition (Büchel, Wise, Mummery, Poline, & Friston, 1996). In particular, kinematic error was quantified as the maximum perpendicular hand-path deviation from a straight line connecting the start position and target (deviation predictor). Trial-specific kinematic error was approximated using the same exponential decay for all FF 7-movement series (see Figure 1C). The predictors obtained by convolution with the SPM5 canonical HRF are presented in Figure 1D. In addition to the two "reach-observation predictors" (one for each NF and FF conditions; "NF-reach-observation" and "FF-reach-observation") and the deviation predictor (for the FF condition), we included in the design matrix, as potentially confounding covariates, the six head-movement parameters resulting from realignment. The scrambled (S) baseline condition was not explicitly modeled.

Contrast images of each subject generated with a fixed-effects model were taken into the group analysis using a random-effects model. The activations reported survived a voxel-level threshold of $p < .001$ (uncorrected) and a cluster-level threshold of $p < .05$ (corrected for multiple comparisons). The SPM5 coordinates were converted from MNI into Talairach coordinates using a nonlinear transform (http://imaging.mrc-cbu.cam.ac.uk/imaging/MniTalairach). As this transformation increases the disparity between the two coordinate systems in some brain regions (Lancaster et al., 2007), we report both MNI and Talairach coordinates throughout the article.

Region-of-Interest Analysis

To investigate the time course within regions involved in reaching observation, we performed an ROI analysis. Data (unsmoothed normalized functional images) were further processed with the SPM extension, MarsBaR (http://marsbar.sourceforge.net/). In each subject, we defined ROIs using the contrast [NF-reach-observation + FF-reach-observation] versus baseline. ROIs included all significant voxels ($p < .001$ uncorrected) within a 10-mm-radius sphere centered on each maximum. For each subject's ROI, a median percent BOLD signal change value (median %BSC) was calculated for the NF and FF conditions and averaged across all eight runs. We then conducted a 2-Force-field movie (FF, NF) by 2-Epoch phase (early, late) repeated measures ANOVA ($\alpha = .05$) on the %BSC measures, with the hypothesis that error-related areas would show an interaction such that the difference between FF and NF would be larger for the early (high FF error observation) rather than the late (low FF error observation) epoch.

RESULTS

Whole-brain Analyses

We first identified areas that showed significant activation during observation of reaching movements (without regard for the perturbation) using the contrast [NF-reach-observation + FF-reach-observation] versus baseline. Activations are shown in violet in Figure 2. Table 1A lists the main peaks of activation that survived a voxel-level threshold of $p < .001$ (uncorrected) and a cluster-level threshold of $p < .05$ (corrected). High levels of activation were found bilaterally in temporo-occipital cortex, with the highest peak for this effect located in the right hemisphere. The extent of activation, however, was more prominent in the left hemisphere. Three main peaks of activation were identified in parieto-occipital cortex, anterior parietal cortex (aPC), and at the "L-junction" of superior frontal and precentral sulci, corresponding to dorsal premotor cortex (PMd). This frontal activation extended inferiorly and laterally into central sulcus and anteriorly to medial frontal gyrus. Left inferior temporal cortex also showed a cluster of activation. Parietal activation was observed in both hemispheres, with a peak in right superior parietal cortex that extended medially into precuneus. Temporo-parietal junction (TPJ) cortex was also activated bilaterally. On the right side, activation was also found within right inferior frontal gyrus, cuneus, and cerebellar cortex (not shown; most likely Crus I given the MNI coordinates and the normalization algorithm used. For a new probabilistic atlas of the cerebellum,

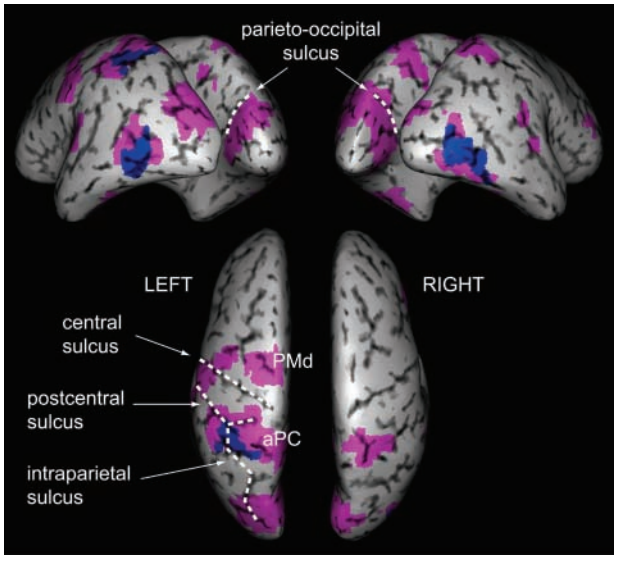

Figure 2. Whole-brain analyses shown on the cortical surface of a representative subject. In violet are areas activated during observation of reaching movements in either the FF or NF conditions. In blue are regions that also exhibited patterns of activation positively correlated with the deviation predictor. For both effects: voxel-level threshold of $p < .001$, uncorrected for multiple comparisons, and a cluster-level threshold of $p < .05$, corrected.

Table 1. Areas Activated during Observation

			MNI Coordinates			*Talairach Coordinates*		
Area	*Side*	*Z Score*	*x*	*y*	*z*	*x*	*y*	*z*
(A) Areas Activated during Reach Observation								
Temporo-occipital	R	6.27	41	−79	6	41	−76	9
Parieto-occipital	L	5.79	−28	−79	24	−28	−75	26
aPC	L	5.78	−34	−38	48	−34	−35	46
PMd	L	5.15	−21	−14	54	−20	−11	50
Inferior temporal	L	5.11	−41	−34	−18	−41	−34	−13
Cuneus	R	5.10	3	−76	24	3	−73	26
Temporo-occipital	L	5.02	−48	−76	0	−48	−74	4
Posterior parietal	R	4.76	21	−48	60	21	−44	57
Cerebellar Crus I	R	4.73	38	−55	−30	38	−55	−23
TPJ	L	4.55	−45	−31	12	−44	−29	13
IFG	R	4.45	52	17	18	52	17	16
TPJ	R	3.56	52	−38	6	51	−37	7
(B) Areas Activated during Reach Observation and Whose Activation Profiles Positively Correlated with the Reach Kinematic Error								
Temporo-occipital	R	6.27	41	−79	6	41	−76	9
aPC	L	5.77	−34	−41	54	−34	−37	52
Temporo-occipital	L	5.02	−48	−76	0	−48	−74	4
PMd	L	4.70	−21	−10	54	−21	−7	50
Cerebellar Crus I	R	4.25	38	−58	−30	38	−57	−22

(A) Main peaks of activation during reaching observation in the voxelwise analysis (voxel-level threshold of $p < .001$, uncorrected, and a cluster-level threshold of $p < .05$, corrected). For clusters including several activation peaks, we list maxima more than 25 mm apart with $Z > 4.60$. (B) Areas activated by reach observation and whose level of activation correlated positively with the amplitude of the hand-path deviation in the voxelwise analysis.

see: http://www.bangor.ac.uk/~pss412/propatlas.htm; Diedrichsen, Balsters, Flavell, Cussans, & Ramnani, 2009).

Ultimately, we were interested in areas that were activated not only by reaching observation but also by kinematic errors during reaching, therefore we focused on the regions that, in addition to being recruited during reach observation, exhibited activation that correlated positively with the amplitude of the observed kinematic error. For this purpose, we defined a mask including all voxels showing patterns of activation positively correlated with the deviation predictor (with a voxel-level threshold of $p < .001$, uncorrected). Peaks of the clusters identified by the mask that also survived the reach-observation contrast, defined as the contrast [NF-reach-observation + FF-reach-observation] versus baseline (at a voxel-level threshold of $p < .001$, uncorrected, and a cluster-level threshold of $p < .05$, corrected), are indicated in blue in Figure 2 and listed in Table 1B; namely, in left intraparietal sulcus (IPS), temporo-occipital cortex bilaterally, and right cerebellum (not shown). Left PMd, although significant at the voxel level ($p = .022$, family-wise error rate-corrected), did not reach significance as a cluster ($p = .258$, corrected).

In SPM5, applying the deviation-predictor inclusive mask before identifying the voxels showing reach-observation activation or proceeding in the reverse order—applying the reach-observation inclusive mask before identifying deviation-predictor related activation—identifies the same set of clusters. The only difference between the two ways to proceed is that by applying the deviation predictor first, you obtain the *t*-(*z*-values) for the reach-observation contrast, whereas by applying the reach-observation mask first, you get the *t*-(*z*-values) for the deviation-predictor effect. Here, we chose to apply the deviation-predictor inclusive mask first to be consistent with the following ROI analysis. Indeed, we defined our ROIs by selecting the voxels showing reach-observation activation and that were 10 mm distant from peaks of activation for this contrast ([NF-reach-observation + FF-reach-observation] vs. baseline).

We do not report any results relative to the contrast FF–NF, as this effect did not reveal any significant cluster of activation (see next section).

Region-of-Interest Analysis

In each individual, ROIs were defined on the basis of the reach-observation effect ([NF-reach-observation + FF-reach-observation] vs. baseline). In Figure 3, we present the data from the subset of regions whose activation profiles were positively correlated with the observed kinematic error, as revealed by the whole-brain analysis. Although the areas that are presented are those that were positively correlated with the observed kinematic error (Table 1B), these ROIs, in terms of the voxels that they contained, were defined entirely by the [NF-reach-observation + FF-reach-observation] versus baseline contrast.

Indeed, although the voxelwise correlation of these five regions with the amplitude of the observed error was suggestive, it is possible that this correlation was not related to processing observed kinematic error, but simply due to habituation (e.g., Grill-Spector, Henson, & Martin, 2006). However, habituation would be expected to affect the NF and FF conditions equally. In fact, if anything, habituation should be stronger for the NF epochs, in which all movements were very similar to each other. In contrast, if the decay of activation was related to error processing, we would expect a larger difference between FF and NF conditions for the early trials in the epoch compared to the later trials.

To test whether there was a larger difference between FF and NF conditions during early compared to late phases of the epoch, we compared the time-course activity (specifically the median %BSC) in these two phases. The graphs in Figure 3 show the average (across-subjects) time courses associated with the FF and the NF conditions. For each subject we calculated the mean (of the median %BSC) activation early (over Scans 4–7) and late (over Scans 13–16) in the 32-sec video clip (Figure 3). We then conducted a 2-Force-field movie (FF, NF) by 2-Epoch phase (early, late) repeated measures ANOVA on these values, with the hypothesis that error-related areas would show an interaction such that the difference between FF and NF would be larger for the early rather

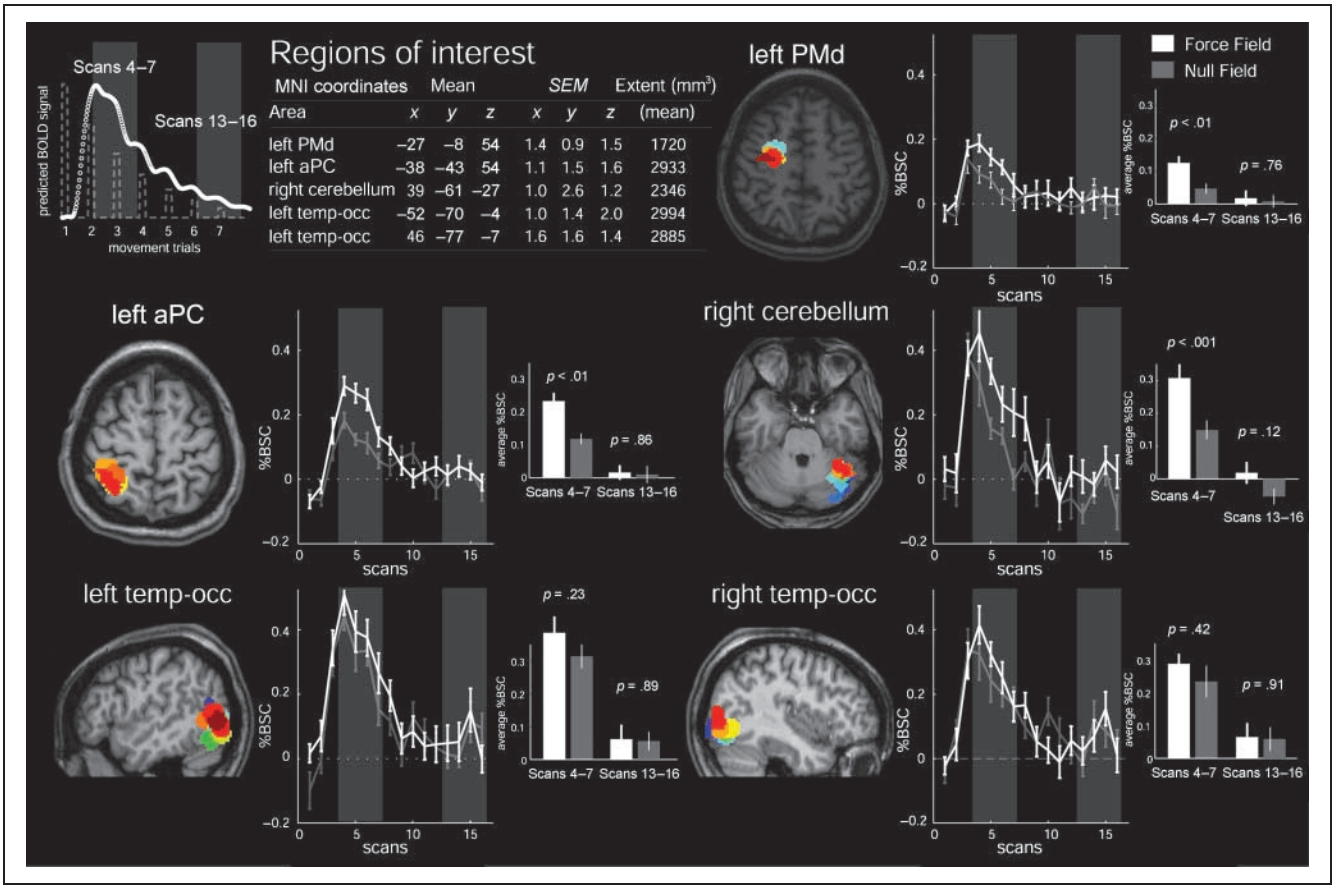

Figure 3. ROIs for different subjects are in different colors, on the anatomy of a single individual. For each subject, a mean activation time course was computed from all runs for each NF and FF conditions. The graphs present the mean ROI activation time courses (±*SEM*) across subjects for the NF and FF. Inset bar-charts show the means (±*SEM*) across subjects averaged over Scans 4–7 (three most deviated movements) and Scans 13–16 (three least deviated movements). The top leftmost panel illustrates the predicted BOLD signal over the 32-sec FF epoch, based on the convolved stick predictors scaled for movement deviation. For each subject, each ROI, and each run, data were realigned by subtracting the mean of all the scans of the run; the $y = 0$ baseline on the time-course graphs corresponds to the mean of all conditions.

than the late epoch. Interaction effects were significant for left aPC [$F(1, 13) = 10.63$, $p < .01$], right cerebellum [$F(1, 13) = 5.40$, $p < .05$], and marginal for left PMd [$F(1, 13) = 3.37$, $p < .09$]. By contrast, no interaction effects were observed for the right and left occipito-temporal regions [$F(1, 13) = 0.89$, $p = .36$, and $F(1, 13) = 1.17$, $p = .30$, respectively]. The lack of an interaction effect in occipito-temporal cortex is an important finding, as it bears on the issue of the visual salience of FF-perturbed (hence, curved) vs. unperturbed (hence, straight) hand-paths (see Discussion). We performed planned comparisons (paired t tests) to compare FF and NF activation in the early phase and in the late phase. Figure 3 presents these results for each ROI.

In the whole-brain voxelwise analysis, the contrast of NF versus FF did not reveal any significant clusters of activation. This is not surprising given that the difference between the two conditions was mainly restricted to the early trials. Also note that all of these comparisons (NF−FF) were independent of the contrast (NF-reach-observation + FF-reach-observation) vs. baseline. More importantly, although all of these ROIs were selected (but not defined) on the basis of their positive correlation with kinematic error, this test allowed us to learn that three of these ROIs were sensitive to reach error (left aPC, left PMd, and right cerebellum), whereas two others were not (left and right temporo-occipital cortex). That is, we could make a discrimination that we could not have made on the basis of the deviation parameter effect alone. This illustrates the independence of the information captured by the ANOVA from the information captured by the deviation correlation.

DISCUSSION

Our goal was to explore the neural network involved in processing visual information about reaching errors committed by others. We used fMRI to record neural activity in subjects watching videos showing another person learning to reach under altered dynamical conditions. Fronto-parietal regions that are normally recruited in active reaching were activated during observation of reaching movements (vs. scrambled versions with similar stimulus motion). Moreover, it appeared that part of the network that has been shown to be engaged in processing self-generated reach error (Diedrichsen, Hashambhoy, Rane, & Shadmehr, 2005) is also involved in observing reach errors committed by others.

Observing Reaching Movements Activates Areas Engaged in Active Reaching

Consistent with past studies of active arm movements (reaching, pointing, and joystick movements), we found significant clusters in parieto-occipital cortex, IPS, and PMd. These results are consistent with other recent comparisons between active and observed reaching movements (Filimon et al., 2007). Stronger activation was observed contralateral to the arm shown in the movies. First, we observed activation in aPC, near the junction of postcentral and intraparietal sulci (Culham et al., 2003) and extending medially from IPS into superior parietal lobule and precuneus (Prado et al., 2005; Grefkes, Ritzl, Zilles, & Fink, 2004). This focus likely includes both the areas that have been proposed as the human functional equivalents of macaque areas involved in reaching, MIP (in humans: hMIP, medial to the IPS; Grefkes & Fink, 2005; Grefkes et al., 2004), and grasping, AIP (in humans: hAIP, in the anterior IPS; Culham et al., 2003; Binkofski et al., 1998). Although comparisons between studies suggest that hMIP is medial, posterior, and superior to AIP (as reviewed in Culham, Cavina-Pratesi, & Singhal, 2006; Grefkes & Fink, 2005), AIP responds strongly to reaching as well as grasping, and to date, distinctions between the areas have not been clearly demonstrated. Second, we observed activation of a cluster in PMd, in agreement with previous imaging studies of active reaching (Diedrichsen et al., 2005; Prado et al., 2005; for a review, see Chouinard & Paus, 2006). Third, we observed activation in superior parieto-occipital cortex, consistent with other studies on reaching and pointing (as reviewed in Culham, Gallivan, Cavina-Pratesi, & Quinlan, 2008), and extending laterally and medially.

The activation that we found in cerebellar cortex, ipsilateral to the observed hand, is consistent with reach related activity found in ipsilateral anterior cerebellum (Diedrichsen et al., 2005). Indeed, areas in ipsilateral lobules V–VI and bilaterally lobule VIII have been shown to have reciprocal connection with primary motor cortex (Kelly & Strick, 2003). Furthermore, activity in cerebellum during action observation agrees with results that extend to the cerebellar structures the observation/execution matching mechanism proposed for cortical areas (for a review, see Petrosini et al., 2003).

We also found strong reach-observation related activity in temporo-occipital cortex slightly posterior and inferior to the human motion complex, V5+ or MT+ (Dumoulin et al., 2000). Although this activation includes MT+, the stereotaxic focus is more consistent with the object-selective lateral occipital cortex, which we would expect to be activated because the reaching observation movements included coherent images versus their scrambled counterparts, a contrast that reliably identifies LOC (Grill-Spector, Kourtzi, & Kanwisher, 2001).

Observing Kinematic Errors in Others' Reaching Movements Engages Regions Involved in Processing Self-generated Reach-execution Errors

The main goal of our study was to identify the neural network involved in processing visual information about

reach errors committed by others. We reasoned that areas whose levels of activation were modulated by the amplitude of observed kinematic errors may also be implicated in correction processes that in active reaching drive adaptation to novel limb-movement dynamics. Activity in frontal and parietal regions, as well as in cerebellum, correlated positively with our hand-path deviation predictor.

Our ROI analyses confirmed that neural activity in aPC and PMd was influenced by visual signals of kinematic error. Indeed, these regions exhibited different levels of activation during observation of the first three reaches performed in the FF condition (most perturbed movements) than during observation of NF-non-deviated reaches, a difference that was not observed for the later trials. Although the interaction for PMd was less robust than for aPC, the pattern was consistent with an error-processing account. It may be that this region did not reach significance in the cluster-thresholded voxelwise analysis because the effect was smaller than in aPC or because the region was smaller and more variable in stereotaxic space.

Interestingly, this pattern of activation appears to converge with the findings of Diedrichsen et al. (2005), who investigated neural activity related to self-generated reach errors. These authors found strong modulation by execution errors in aPC bilaterally with the highest peak left-lateralized (MNI coordinates: $x = -30, y = -45, z = 66$ and $x = 37, y = -38, z = 52$), and right (ipsilateral) cerebellar cortex. Likewise, in the present study, the ROIs identified in ipsilateral cerebellar cortex exhibited highest activation during most perturbed FF movements, which is consistent with a large body of evidence suggesting an important role of cerebellum in adaptive signal-error processing (e.g., Zhang, Forster, Milner, & Iadecola, 2003; Imamizu et al., 2000; Smith, Brandt, & Shadmehr, 2000; Kitazawa, Kimura, & Yin, 1998). Thus, although Petrosini et al. (2003) demonstrated a role of cerebellum in learning by observation about movement selection, our results indicate that it may also be involved in learning by observing about movement execution. Although the work cited above examined the neural correlates of error production, the current study addressed only error observation. Nevertheless, the overlap in patterns of activation across these studies is consistent with the idea that these brain regions are involved in the visual processing of reaching errors more generally—whether generated or observed.

We have identified here a number of brain regions in which neural activity is modulated by kinematic error (signaled by movement curvature). One possibility is that these regions are not processing kinematic error per se, but are responding to the visual aspects of curved movement paths. However, an examination of the pattern of results for temporo-occipital regions, which are known to be sensitive to visual salience (Downar, Crawley, Mikulis, & Davis, 2002), argues against this possibility. Specifically, although activity in temporo-occipital regions was modulated over time, and thus, generally correlated with the kinematic error predictor, there were no differences in activation between NF and FF trials (Figure 3). This was the case even for early trials in which observed kinematic error (hence, movement curvature) was much greater in FF versus NF conditions, suggesting that FF perturbed reaches were not simply more interesting or visually salient than the NF reaches.

Another related possibility is that activation differences between FF and NF trials may have been driven by attentional factors rather than effects of visuomotor processing. Again, this seems unlikely, given that brain regions showing significant correlations with hand-path deviations were not observed bilaterally, as would be expected if these effects were based on attentional factors (Wojciulik & Kanwisher, 1999). Rather, these activations were primarily left-lateralized in parietal and right-lateralized in cerebellar cortex.

Although our results suggest that fronto-parietal and cerebellar structures that are involved in processing self-generated reach errors (Diedrichsen et al., 2005) may also be engaged in processing observed kinematic errors, our study does not address the question of whether or not information about movement dynamics is conveyed visually. Indeed, Diedrichsen et al. (2005), who explored neural activation associated with active reaching errors, found that execution errors induced by rotation of the visual display and execution errors due to misestimation of the dynamics of the task drive activation in similar neural networks. Thus, the possibility remains that for "genuine" dynamic learning to occur, somatosensory feedback is needed. Indeed, this would be consistent with the fact that FF learning by observing is largely partial (Mattar & Gribble, 2005). This interpretation also fits with results indicating that parietal area 5 (Kalaska, Cohen, Prud'homme, & Hyde, 1990) and premotor cortex primarily encode movement kinematics rather than movement dynamics.

In regard to previous findings that demonstrated the role of the primary motor (M1) cortex in FF adaptation (Cothros, Köhler, Dickie, Mirsattari, & Gribble, 2006; Li, Padoa-Schioppa, & Bizzi, 2001; Gandolfo, Li, Benda, Schioppa, & Bizzi, 2000), one may be surprised that we found central sulcus activation to relate to observation of reaching movements but not specifically to observed kinematic error. Again, it is interesting to note that Diedrichsen et al. (2005) also do not report error-processing-related activation in M1. These authors conjecture that modulation in M1 might indeed require a coherent adaptation process, rather than discrete error processing. In the present study, it seems reasonable that the fractionated nature of the FF movies (required for the current fMRI experimental design) may have reduced the opportunity for coherent motor learning to occur.

Acknowledgments

This work was supported by the Natural Sciences and Engineering Research Council of Canada, the Canadian Institutes of

Health Research (200409MOP-BSC-134162-A), and the National Institutes of Health (USA). We thank Jeremy Wong and Elizabeth T. Wilson for their help in creating the movies.

Reprint requests should be sent to Nicole Malfait, UMR 6149 Neurosciences Intégratives et Adaptatives, CNRS, Centre St Charles, Pôle 3C-Case B, 3, Place Victor Hugo, 13331 Marseille Cedex 03, France, or via e-mail: nmalfait@gmail.com.

REFERENCES

Binkofski, F., Dohle, C., Posse, S., Stephan, K. M., Hefter, H., Seitz, R. J., et al. (1998). Human anterior intraparietal area subserves prehension: A combined lesion and functional MRI activation study. *Neurology, 50,* 1253–1259.

Blandin, Y., & Proteau, L. (2000). On the cognitive basis of observational learning: Development of mechanisms for the detection and correction of errors. *Quarterly Journal of Experimental Psychology: Human Experimental Psychology, 53A,* 846–867.

Büchel, C., Wise, R. J. S., Mummery, C. J., Poline, J.-B., & Friston, K. J. (1996). Nonlinear regression in parametric activation studies. *Neuroimage, 4,* 60–66.

Chong, T. T., Cunnington, R., Williams, M. A., Kanwisher, N., & Mattingley, J. B. (2008). fMRI adaptation reveals mirror neurons in human inferior parietal cortex. *Current Biology, 18,* 1576–1580.

Chouinard, P. A., & Paus, T. (2006). The primary motor and premotor areas of the human cerebral cortex. *Neuroscientist, 12,* 143–152.

Cothros, N., Köhler, S., Dickie, E. W., Mirsattari, S. M., & Gribble, P. L. (2006). Proactive interference as a result of persisting neural representations of previously learned motor skills in primary motor cortex. *Journal of Cognitive Neuroscience, 18,* 2167–2176.

Cross, E. S., Kraemer, D. J., Hamilton, A. F., Kelley, W. M., & Grafton, S. T. (2009). Sensitivity of the action observation network to physical and observational learning. *Cerebral Cortex, 19,* 315–326.

Culham, J. C., Cavina-Pratesi, C., & Singhal, A. (2006). The role of parietal cortex in visuomotor control: What have we learned from neuroimaging? *Neuropsychologia, 44,* 2668–2684.

Culham, J. C., Danckert, S. L., DeSouza, J. F., Gati, J. S., Menon, R. S., & Goodale, M. A. (2003). Visually guided grasping produces fMRI activation in dorsal but not ventral stream brain areas. *Experimental Brain Research, 153,* 180–189.

Culham, J. C., Gallivan, J., Cavina-Pratesi, C., & Quinlan, D. J. (2008). fMRI investigations of reaching and ego space in human superior parieto-occipital cortex. In R. L. Klatzky, M. Behrmann, & B. MacWhinney (Eds.), *Embodiment, ego-space and action* (pp. 247–274). New York: Psychology Press.

Di Pellegrino, G., Fadiga, L., Fogassi, L., Gallese, V., & Rizzolatti, G. (1992). Understanding motor events: A neurophysiological study. *Experimental Brain Research, 91,* 176–180.

Diedrichsen, J., Balsters, J. H., Flavell, J., Cussans, E., & Ramnani, N. (2009). A probabilistic MR atlas of the human cerebellum. *Neuroimage, 46,* 39–46.

Diedrichsen, J., Hashambhoy, Y., Rane, T., & Shadmehr, R. (2005). Neural correlates of reach errors. *Journal of Neuroscience, 25,* 9919–9931.

Diedrichsen, J., & Shadmehr, R. (2005). Detecting and adjusting for artifacts in fMRI time series data. *Neuroimage, 27,* 624–634.

Dinstein, I., Thomas, C., Behrmann, M., & Heeger, D. J. (2008). A mirror up to nature. *Current Biology, 18,* R13–R18.

Dizio, P., & Lackner, J. R. (1995). Motor adaptation to Coriolis force perturbations of reaching movements: Endpoint but not trajectory adaptation transfers to thenon-exposed arm. *Journal of Neurophysiology, 74,* 1787–1792.

Dizio, P., & Lackner, J. R. (2000). Congenitally blind individuals rapidly adapt to Coriolis force perturbations of their reaching movements. *Journal of Neurophysiology, 84,* 2175–2180.

Downar, J., Crawley, A. P., Mikulis, D. J., & Davis, K. D. (2002). A cortical network sensitive to stimulus salience in a neutral behavioural context across multiple sensory modalities. *Journal of Neurophysiology, 87,* 615–620.

Dumoulin, S. O., Bittar, R. G., Kabani, N. J., Baker, C. L., Jr., Le Goualher, G., Bruce Pike, G., et al. (2000). A new anatomical landmark for reliable identification of human area V5/MT: A quantitative analysis of sulcal patterning. *Cerebral Cortex, 10,* 454–463.

Fadiga, L., Craighero, L., & Olivier, E. (2005). Human motor cortex excitability during the perception of others' action. *Current Opinion in Neurobiology, 15,* 213–218.

Filimon, F., Nelson, J. D., Hagler, D. J., & Sereno, M. I. (2007). Human cortical representations for reaching: Mirror neurons for execution, observation, and imagery. *Neuroimage, 37,* 1315–1328.

Flanagan, J. R., & Johansson, R. (2003). Action plans used in action observation. *Nature, 424,* 769–771.

Friston, K. J., Rotshtein, P., Geng, J. J., Sterzer, P., & Henson, R. N. (2006). A critique of functional localisers. *Neuroimage, 30,* 1077–1087.

Gallese, V., Fadiga, L., Fogassi, L., & Rizzolatti, G. (1996). Action recognition in the premotor cortex. *Brain, 119,* 593–609.

Gandolfo, F., Li, C., Benda, B. J., Schioppa, C. P., & Bizzi, E. (2000). Cortical correlates of learning in monkeys adapting to a new dynamical environment. *Proceedings of the National Academy of Sciences, U.S.A., 97,* 2259–2263.

Ghez, C., Gordon, J., & Ghilardi, M. F. (1995). Impairments of reaching movements in patients without proprioception: II. Effects of visual information on accuracy. *Journal of Neurophysiology, 73,* 361–372.

Grefkes, C., & Fink, G. R. (2005). The functional organization of the intraparietal sulcus in humans and monkeys. *Journal of Anatomy, 207,* 3–17.

Grefkes, C., Ritzl, A., Zilles, K., & Fink, G. R. (2004). Human medial intraparietal cortex subserves visuomotor coordinate transformation. *Neuroimage, 23,* 1494–1506.

Grill-Spector, K., Henson, R., & Martin, A. (2006). Repetition and the brain: Neural models of stimulus specific effects. *Trends in Cognitive Sciences, 10,* 14–23.

Grill-Spector, K., Kourtzi, Z., & Kanwisher, N. (2001). The lateral occipital complex and its role in object recognition. *Vision Research,* 1409–1422.

Hari, R., Forss, N., Avikainen, S., Kirveskari, E., Salenius, S., & Rizzolatti, G. (1998). Activation of human primary motor cortex during action observation: A neuromagnetic study. *Proceedings of the National Academy of Sciences, U.S.A., 95,* 15061–15065.

Iacoboni, M., Woods, R. P., Brass, M., Bekkering, H., Mazziotta, J. C., & Rizzolatti, G. (1999). Cortical mechanisms of human imitation. *Science, 286,* 2526–2528.

Iacoboni, M., & Mazziotta, J. C. (2007). Mirror neuron system: Basic findings and clinical applications. *Annals of Neurology, 62,* 213–218.

Imamizu, H., Miyauchi, S., Tamada, T., Sasaki, Y., Takino, R., Puetz, B., et al. (2000). Human cerebellar activity reflecting an acquired internal model of a new tool. *Nature, 403,* 192–195.

Kalaska, J. F., Cohen, D. A., Prud'homme, M., & Hyde, M. L. (1990). Parietal area 5 neuronal activity encodes movement kinematics, not movement dynamics. *Experimental Brain Research, 80,* 351–364.

Kelly, R. M., & Strick, P. L. (2003). Cerebellar loops with motor cortex and prefrontal cortex of a nonhuman primate. *Journal of Neuroscience, 23,* 8432–8444.

Kilner, J. M., Friston, K. J., & Frith, C. D. (2007). Predictive coding: An account of the mirror neuron system. *Cognitive Processing, 8,* 159–166.

Kitazawa, S., Kimura, T., & Yin, P. B. (1998). Cerebellar complex spikes encode both destinations and errors in arm movements. *Nature, 392,* 494–497.

Lackner, J. R., & Dizio, P. (1994). Rapid adaptation to Coriolis force perturbations of arm trajectory. *Journal of Neurophysiology, 72,* 299–313.

Lancaster, J. L., Tordesillas-Gutiérrez, D., Martinez, M., Salinas, F., Evans, A., Zilles, K., et al. (2007). Bias between MNI and Talairach coordinates analyzed using the ICBM-152 brain template. *Human Brain Mapping, 28,* 1194–1205.

Li, C. S., Padoa-Schioppa, C., & Bizzi, E. (2001). Neuronal correlates of motor performance and motor learning in the primary motor cortex of monkeys adapting to an external force field. *Neuron, 30,* 593–607.

Maeda, F., Kleiner-Fisman, G., & Pascual-Leone, A. (2002). Motor facilitation while observing hand actions: Specificity of the effect and role of observer's orientation. *Journal of Neurophysiology, 87,* 1329–1335.

Mattar, A. A. G., & Gribble, P. L. (2005). Motor learning by observing. *Neuron, 46,* 153–160.

Petrosini, L., Graziano, A., Mandolesi, L., Neri, P., Molinari, M., & Leggio, M. G. (2003). Watch how to do it! New advances in learning by observation. *Brain Research, Brain Research Reviews, 42,* 252–264.

Prado, J., Clavagnier, S., Otzenberger, H., Scheiber, C., Kennedy, H., & Perenin, M. T. (2005). Two cortical systems for reaching in central and peripheral vision. *Neuron, 48,* 849–858.

Rizzolatti, G., & Craighero, L. (2004). The mirror-neuron system. *Annual Review of Neuroscience, 27,* 169–192.

Rizzolatti, G., & Fabbri-Destro, M. (2008). The mirror system and its role in social cognition. *Current Opinion in Neurobiology, 18,* 179–184.

Rizzolatti, G., Fogassi, L., & Gallese, V. (2001). Neurophysiological mechanisms underlying the understanding and imitation of action. *Nature Reviews Neuroscience, 2,* 661–670.

Sainburg, R. L., Ghez, C., & Kalkanis, D. (1999). Intersegmental dynamics are controlled by sequential anticipatory error correction and postural mechanisms. *Journal of Neurophysiology, 81,* 1045–1056.

Sainburg, R. L., Ghilardi, M. F., Poizner, H., & Ghez, C. (1995). Control of limb dynamics in normal subjects and patients without proprioception. *Journal of Neurophysiology, 73,* 820–835.

Saxe, R., Brett, M., & Kanwisher, N. (2006). Divide and conquer: A defense of functional localizers. *Neuroimage, 30,* 1088–1096.

Scheidt, R. A., Conditt, M. A., Secco, E. L., & Mussa-Ivaldi, F. A. (2005). Interaction of visual and proprioceptive feedback during adaptation of human reaching movements. *Journal of Neurophysiology, 93,* 3200–3213.

Scheidt, R. A., Reinkensmeyer, D. J., Conditt, M. A., Rymer, W. Z., & Mussa-Ivaldi, F. A. (2000). Persistence of motor adaptation during constrained, multi-joint, arm movements. *Journal of Neurophysiology, 84,* 853–862.

Shadmehr, R., & Mussa-Ivaldi, F. A. (1994). Adaptive representation of dynamics during learning of a motor task. *Journal of Neuroscience, 14,* 3208–3224.

Shmuelof, L., & Zohary, E. (2007). Watching others' actions: Mirror representations in the parietal cortex. *Neuroscientist, 13,* 667–672.

Smith, M. A., Brandt, J., & Shadmehr, R. (2000). Motor disorder in Huntington's disease begins as a dysfunction in error feedback control. *Nature, 403,* 544–549.

Sober, S. J., & Sabes, P. N. (2003). Multisensory integration during motor planning. *Journal of Neuroscience, 23,* 6982–6992.

Van Schie, H. T., Mars, R. B., Coles, M. G., & Bekkering, H. (2004). Modulation of activity in medial frontal and motor cortices during error observation. *Nature Neuroscience, 7,* 549–554.

Wojciulik, E., & Kanwisher, N. (1999). The generality of parietal involvement in visual attention. *Neuron, 23,* 747–764.

Zhang, Y., Forster, C., Milner, T. A., & Iadecola, C. (2003). Attenuation of activity induced increases in cerebellar blood flow by lesion of the inferior olive. *American Journal of Physiology: Heart and Circulatory Physiology, 285,* H1177–H1182.